AIAA JOURNAL
Vol. 56, No. 6, June 2018

Technical Notes

Phugoid Motion Simulation of a Supersonic Transport Using Navier–Stokes Equations

Guru Guruswamy*
NASA Ames Research Center, Moffett Field, California 94035

DOI: 10.2514/1.J056653

Nomenclature

C_D	=	coefficient of total drag
C_L	=	coefficient of total lift
C_P	=	coefficient of pressure
g	=	acceleration due to gravity, ft/s^2
M	=	Mach number
Q	=	dynamic pressure, lb/ft^2
S	=	surface area, ft^2
u	=	perturbation velocity, ft/s
u_0	=	initial velocity, ft/s
V	=	flight-path velocity vector
α	=	angle of attack, deg
θ	=	pitch angle, deg

I. Introduction

THERE is a renewed interest in developing new supersonic transports [1] after the discontinuation of the Concorde supersonic jet [2], which was mostly limited for flights over transoceanic routes due to the severe noise of sonic boom. To avoid the sonic boom, more slender configurations such as the low-boom flight demonstrator configuration [3] are being considered. Supersonic transports tend to have different stability issues than conventional subsonic transports. For example, the 67 deg swept supersonic configuration of the B-1 aircraft experienced leading-edge vortex-induced aeroelastic oscillations [4] that are not observed for conventional subsonic aircraft. The first bending mode frequency of the fuselage of a slender supersonic configuration is closer to the first bending mode frequency of the wing [5] that may lead to unstable coupling associated with rigid-body modes.

Assuring stability of supersonic aircraft, particularly during descent from the supersonic Mach regime to the transonic regime, is important. An aircraft can deviate from its normal descent trajectory due to coupling between flows and rigid-body motions. One such possibility is an aircraft experiencing phugoid oscillations [6,7], as shown in Fig. 1. Oscillation in the altitude due to the exchange between potential energy and kinetic energy is called phugoid oscillation. Beginning at the bottom of the cycle, pitch angle θ increases as the aircraft gains altitude and loses forward speed V. During phugoid motion, the angle of attack α remains constant so that a drop in forward speed amounts to a decrease in lift and flattening of the pitch attitude. As a result, the pitch angle goes to zero at the top of the cycle. Beyond this point, the aircraft begins to lose altitude, the pitch angle goes negative, and airspeed increases. At the bottom of the cycle, the attitude levels, and the airspeed is at its maximum.

To date, usually linear aerodynamic theory-based computational methods with corrections from wind-tunnel data are used to simulate phugoid motions [6]. The phugoid equation formulation in Eqs. (1–3) [7] shows that the damping of the motion depends on lift and drag coefficients, including their gradients with Mach numbers. Such gradients are steep and nonlinear in the transonic regime and cannot be computed adequately by using the linear theory.

Therefore, one should use the well-established Reynolds-averaged Navier–Stokes (RANS) equations that are computationally feasible with current supercomputers.

Use of RANS equations to simulate fluid–structure interaction problems, including trajectory motions, is well advanced [8,9]. In this paper, the trajectory equations associated with phugoid motion are integrated with RANS equations, and results are demonstrated for a supersonic transport aircraft.

II. Approach

Following the derivations in [7], assuming that the phugoid motion starts with level flight, the equations of motion are written as

$$\frac{\mathrm{d}}{\mathrm{d}t}\begin{Bmatrix} u \\ \theta \end{Bmatrix} = \begin{bmatrix} X_u - g \\ \frac{-Z_u}{u_0} \quad 0 \end{bmatrix}\begin{Bmatrix} u \\ \theta \end{Bmatrix} \tag{1}$$

where u is the change in the velocity from the initial velocity u_0, θ is the flight-path angle, and g is acceleration due to gravity. X_u and Z_u are defined as

$$X_u = -\frac{QS}{mu_0}[2C_{L0} + MC_{LM}] \tag{2}$$

$$Z_u = -\frac{QS}{mu_0}[2C_{D0} + MC_{DM}] \tag{3}$$

where Q is the dynamic pressure, S is the reference area, m is mass, C_{L0} is the initial lift coefficient, C_{D0} is the initial drag coefficient, M is that Mach number, and $C_{LM} = \frac{\partial C_L}{\partial M}$ and $C_{DM} = \frac{\partial C_D}{\partial M}$ are rates of change of lift and drag coefficients with Mach number, respectively.

Equation system (1) is combined into a single ordinary differential equation with u as a variable by using $\theta = (X_u u - \dot{u})/g$, which results in

$$\ddot{u} - X_u\dot{u} - \frac{Z_u g}{u_0}u = 0.0 \tag{4}$$

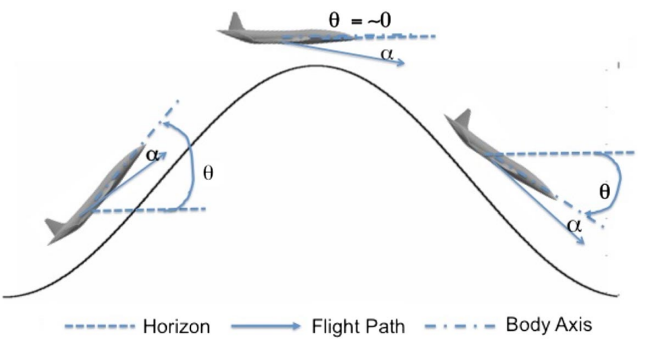

Fig. 1 Trajectory path of aircraft during phugoid oscillation.

Received 24 August 2017; revision received 4 December 2017; accepted for publication 6 December 2017; published online 30 March 2018.

*Senior Aerospace Engineer, Computational Physics Branch. Associate Fellow AIAA.

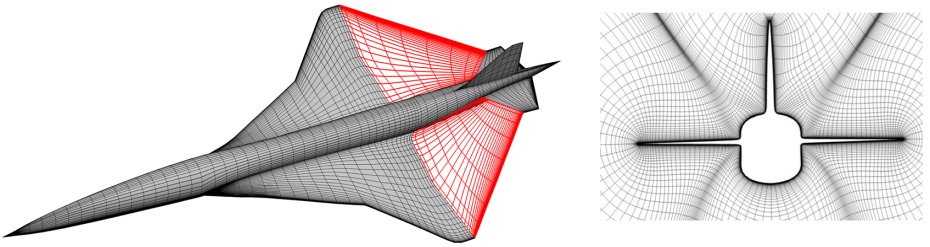

a) b)

Fig. 2 Grids: a) surface and wake (red) grids of a typical supersonic transport, and b) section grid at the tail.

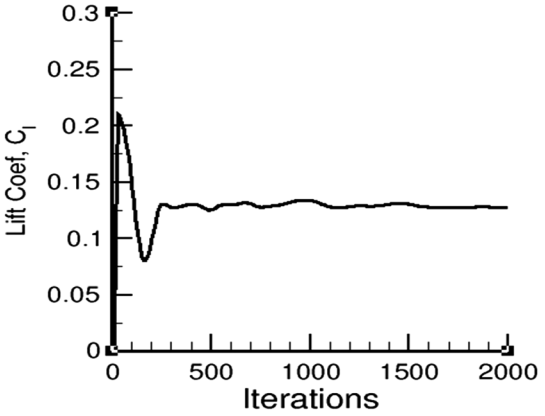

Fig. 3 Convergence of lift coefficient at $M = 0.95, \alpha = 5$ deg.

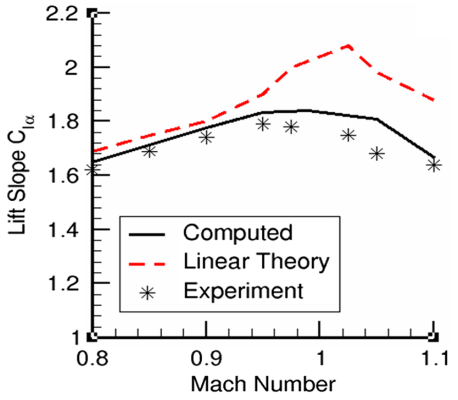

Fig. 4 Comparison of lift coefficient slopes at $\alpha = 5$ deg.

In this work, Eq. (4) is solved using Newmark's time integration method in association with the instantaneous Lagrangian–Eulerian approach (known as arbitrary Lagrangian–Eulerian) [8], with the aerodynamic data computed by solving RANS equations [10]. For this work, the RANS equations are numerically solved using OVERFLOW code [11], which uses the diagonal form of the Beam–Warming central difference algorithm [12], along with the one-equation Spalart–Allmaras turbulence model [13].

Starting from the steady-state converged solution for a given Mach number, time integration of Eq. (4) is initiated. Using the perturbation velocity u at every step computed from Eq. (4), the new Mach number is obtained for the next time step. From u, the pitch angle and altitude are computed. Because the angle of attack remains constant and change in the altitude is negligible, only Mach number needs to be changed in the RANS code at every step.

III. Results

A generic supersonic transport conceived by NASA Langley Research Center [14] is selected for demonstration because it exists in the public domain. A grid that satisfies engineering requirements such as in spacing and stretching factors is selected [15]. Figure 2 shows alternate grid lines of the surface grid including the wake grid (red) defined by 174 points in the axial direction (x) and 422 points in the circumferential direction (y–z) and near-body section grid at the tail. With H-O topology (where H means stacked as surfaces in the x direction, and O means each surface wrapped around the body), the outer boundary surfaces are placed at about 15 lengths of the vehicle using 75 grid points. Numerical experiments similar to that reported in [15] were performed for this grid to assess its resolution quality. The selected grid of size $422 \times 174 \times 75$ is found adequate to give acceptable force quantities needed for this work. For example, at $M = 0.95$ and $\alpha = 5$ deg, computation with 211 points in the y direction changed C_L and C_D by 0.625 and 1.55%, respectively.

Figure 3 shows the typical convergence of lift coefficient within 2000 iterations. Figure 4 shows the comparison of slope of lift coefficients with experiment and the linear theory [14]. The results from the linear theory deviate from both RANS and experimental

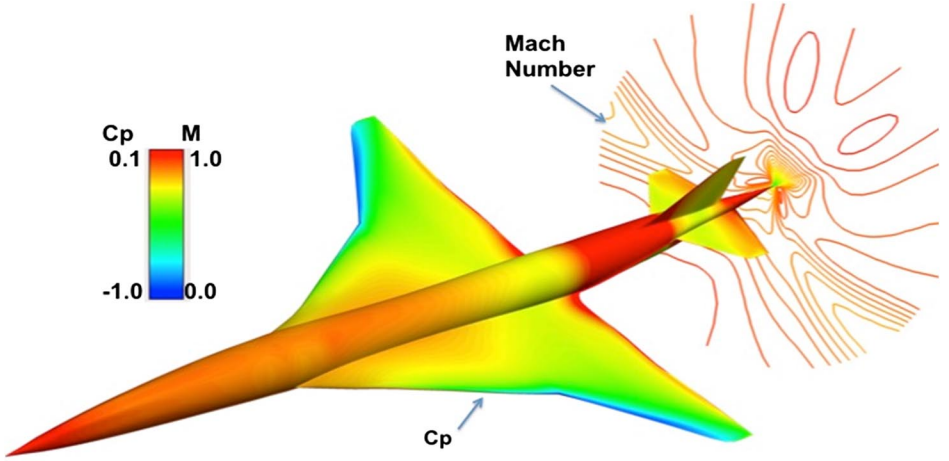

Fig. 5 Surface C_P and tail region Mach number distributions at $M = 0.95, \alpha = 5$ deg.

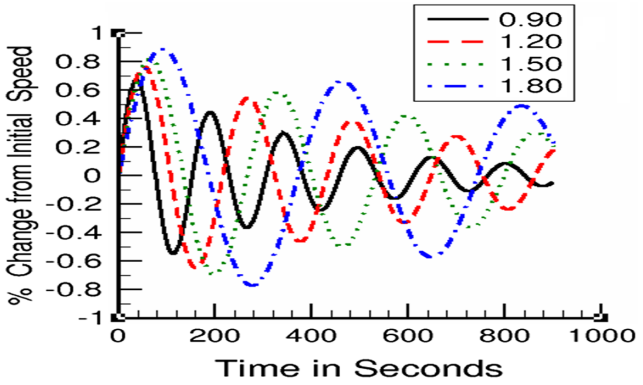

Fig. 6 Effect of Mach numbers on change in speed at $\alpha = 5$ deg.

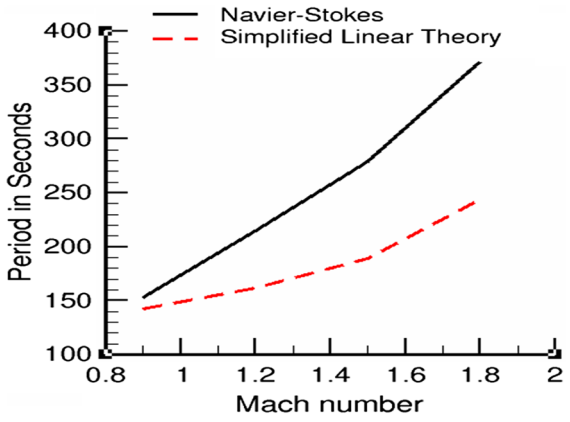

Fig. 7 Effect of Mach number on oscillation period $\alpha = 5$ deg.

data, particularly in the transonic Mach number range. Figure 5 shows surface C_P and tail-region Mach number distributions. The variation in C_P is less pronounced compared to a subsonic transport due to large leading-edge sweep angles.

By using the surface area and mass of a typical supersonic transport [14], Eq. (4) is solved at various initial Mach numbers. Figure 6 shows the percentage change in the velocity from the initial velocity at various starting Mach numbers. Both amplitude and period of oscillation increase with the Mach number. Figure 7 shows comparison of the period of oscillation with results obtained by the simplified linear theory [7] that neglects compressibility and the effects of change in the Mach number on lift and drag coefficients. Differences are more pronounced at higher Mach numbers.

IV. Conclusions

This work presents a complete time-accurate procedure based on Reynolds-averaged Navier–Stokes (RANS) equations to compute phugoid responses. The procedure presented in this paper will help in the design of highly slender, next-generation supersonic transports. Figures 4 and 7 show the importance of using RANS equations instead of the linear aerodynamic equations. The fully time-accurate approach presented here can be used to check whether aeroelastic oscillations get initiated from rigid-body phugoid motion. Future work involves modeling the flexibility of the vehicle [16] including advanced multibody dynamics modules [17].

Acknowledgments

This work was partially supported under applied research activity of the NASA Advanced Supercomputing Division (NAS), Ames Research Center. The author acknowledges suggestions made by Steven Yoon, Chief of Computational Physics Branch of NAS.

References

[1] "NASA Begins Work to Build Quieter Supersonic Passenger Jet," NASA, Feb. 2016, https://www.nasa.gov/press-release/nasa-begins-work-to-build-a-quieter-supersonic-passenger-jet [retrieved 30 Oct. 2017].

[2] Lawless, J., "Final Concorde Flight Lands at Heathrow," Washington Post, Oct. 2003, http://www.washingtonpost.com/wp-dyn/articles/A11477-2003Oct24.html [retrieved 30 Oct. 2017].

[3] Ordaz, I., Geiselhart, K., and Fenbert, J. W., "Conceptual Design of Low Boom Supersonic Aircraft with Flight Trim Requirement," *32nd AIAA Applied Aerodynamics Conference*, AIAA Paper 2014-2141, June 2014.

[4] Guruswamy, G. P., "Vortical Flow Computations on a Flexible Blended Wing-Body Configuration," *AIAA Journal*, Vol. 30, No. 10, Oct. 1992, pp. 2497–2503. doi:10.2514/3.11252

[5] Sakata, I. F., and Davis, G. W., "Evaluation of Structural Design Concepts of an Arrow-Wing Supersonic Cruise Aircraft," NASA CR 2667, April 1977.

[6] Uso, W., "A Study of the Longitudinal Low Frequency (Phugoid) Motion of an Airplane at Supersonic and Hypersonic Speeds," Ph.D. Thesis, California Inst. of Technology, Pasadena, CA, 1967, http://Resolver.Caltech.Edu/Caltechetd:Etd-11152005-105053 [retrieved 16 March 2018].

[7] Caughey, D. A., "Introduction to Aircraft Stability and Control," Sibley School of Mechanical and Aerospace Engineering, Cornell Univ., Ithaca, NY, 2011, https://courses.cit.cornell.edu/mae5070/Caughey_2011_04.pdf [retrieved 16 March 2018].

[8] Guruswamy, G. P., "Time-Accurate Aeroelastic Computations of a Full Helicopter Model Using the Navier–Stokes Equations," *International Journal of Aerospace Innovations*, Vol. 5, Nos. 3–4, Dec. 2013, pp. 73–82. doi:10.1260/1757-2258.5.3-4.73

[9] Guruswamy, G. P., "Time Accurate Coupling of 3-DOF Parachute System with Navier–Stokes Equations," *Journal of Spacecraft and Rockets*, Vol. 54, No. 6, 2017, pp. 1278–1283.

[10] Peyret, R., and Viviand, H., "Computation of Viscous Compressible Flows Based on Navier–Stokes Equations," AGARD AG-212, Neuilly sur Seine, France, 1975.

[11] Nichols, R. H., Tramel, R. W., and Buning, P. G., "Solver and Turbulence Model Upgrades to OVERFLOW 2 for Unsteady and High-Speed Applications," *24th Applied Aerodynamics Conference*, AIAA Paper 2006-2824, June 2006.

[12] Beam, R. M., and Warming, R. F., "An Implicit Factored Scheme for the Compressible Navier–Stokes Equations," *AIAA Journal*, Vol. 16, No. 4, 1978, pp. 393–402. doi:10.2514/3.60901

[13] Spalart, P. R., and Allmaras, S., "A One-Equation Turbulence Model for Aerodynamic Flows," *30th Aerospace Sciences Meeting and Exhibit*, AIAA Paper 1992-0439, 1992.

[14] Raney, D. L., Jackson, E. B., and Buttrill, C. S., "Simulation Studies of Impact of Aeroelastic Characteristics on Flying Qualities of a High Speed Civil Transport," NASA TP 2002-211943, Oct. 2002.

[15] Guruswamy, G. P., "Dynamic Stability Analysis of Hypersonic Transport During Reentry," *AIAA Journal*, Vol. 54, No. 11, Nov. 2016, pp. 3374–3381. doi:10.2514/1.J055018

[16] Guruswamy, G. P., "Development and Applications of a Large Scale Fluids/Structures Simulation Process on Clusters," *Computers & Fluids*, Vol. 36, No. 3, March 2007, pp. 530–539. doi:10.1016/j.compfluid.2006.03.005

[17] MBDyn, Software Package, Ver. 1.7, https://www.mbdyn.org [retrieved 30 Oct. 2017].

R. K. Kapania
Associate Editor